

American University in Cairo

## AUC Knowledge Fountain

---

Faculty Journal Articles

---

6-23-2023

# Investigation of the Wear Behavior of Dual-Matrix Aluminum–(Aluminum–Carbon Nanotube) Composites

Noha M. Abdeltawab

*Department of Mechanical Design and Production, Faculty of Engineering, Cairo University, Giza 12316, Egypt*

Amal M. K. Esawi

*Department of Mechanical Engineering, The American University in Cairo, AUC Avenue, P.O. Box 74, New Cairo 11835, Egypt*

Abdalla Wifi

*Department of Mechanical Design and Production, Faculty of Engineering, Cairo University, Giza 12316, Egypt*

Follow this and additional works at: [https://fount.aucegypt.edu/faculty\\_journal\\_articles](https://fount.aucegypt.edu/faculty_journal_articles)

---

## Recommended Citation

### APA Citation

Abdeltawab, N. Esawi, A. & Wifi, A. (2023). Investigation of the Wear Behavior of Dual-Matrix Aluminum–(Aluminum–Carbon Nanotube) Composites. *Metals*, 13, 10.3390/met13071167  
[https://fount.aucegypt.edu/faculty\\_journal\\_articles/5346](https://fount.aucegypt.edu/faculty_journal_articles/5346)

### MLA Citation

Abdeltawab, Noha M., et al. "Investigation of the Wear Behavior of Dual-Matrix Aluminum–(Aluminum–Carbon Nanotube) Composites." *Metals*, vol. 13, 2023, [https://fount.aucegypt.edu/faculty\\_journal\\_articles/5346](https://fount.aucegypt.edu/faculty_journal_articles/5346)

This Research Article is brought to you for free and open access by AUC Knowledge Fountain. It has been accepted for inclusion in Faculty Journal Articles by an authorized administrator of AUC Knowledge Fountain. For more information, please contact [fountadmin@aucegypt.edu](mailto:fountadmin@aucegypt.edu).

## Article

# Investigation of the Wear Behavior of Dual-Matrix Aluminum–(Aluminum–Carbon Nanotube) Composites

Noha M. Abdeltawab <sup>1</sup>, Amal M. K. Esawi <sup>2,\*</sup>  and Abdalla Wifi <sup>1</sup>

<sup>1</sup> Department of Mechanical Design and Production, Faculty of Engineering, Cairo University, Giza 12316, Egypt; noha.abdeltwab@aucegypt.edu (N.M.A.); aswafi@eng.cu.edu.eg (A.W.)

<sup>2</sup> Department of Mechanical Engineering, The American University in Cairo, AUC Avenue, P.O. Box 74, New Cairo 11835, Egypt

\* Correspondence: a\_esawi@aucegypt.edu

**Abstract:** Aluminum (Al)–aluminum–carbon nanotube (Al–CNT) dual-matrix (DM) composites are a novel class of nanocomposite materials that combine the ductility of the Al matrix with the hardness and wear resistance of the Al–CNT composite and thus can offer a unique combination of properties that make them suitable for a wide range of wear applications such as cutting tools, bearings, brake pads, wear-resistant coatings, etc. However, the specific properties of the DM Al–(Al–CNT) composite will depend on several factors related to the material’s composition and the friction conditions. This study investigates the wear behavior of DM Al–(Al–CNT) composites consisting of a primary matrix of soft aluminum in which milled hard particles of (Al–CNT) are dispersed as affected by five parameters: (1) wt.% CNT in the reinforcement particles, (2) mixing ratio between the reinforcement particles and the soft Al matrix, (3) sliding speed, (4) applied load, and (5) distance. The experimental design used a Taguchi fractional factorial orthogonal array (OA) L<sub>27</sub> to reduce the number of experiments, and analysis of variance (ANOVA) was used to determine the significance and to model the effect of each control parameter. Results showed that the wear rate could be reduced by up to 80% by tailoring the composition and controlling the friction conditions. It was found that the mixing ratio significantly impacts the wear behavior of DM Al–(Al–CNT) composites. A mixing ratio of 50% and a CNT content of 3 wt.% at the lowest applied load gave the lowest wear rate and coefficient of friction. Scanning electron microscopy investigations showed fragmentations in the reinforced matrix at higher loads and mixing ratios, which negatively impacted the wear behavior. Our findings confirm that DM Al–(Al–CNT) composites are promising for wear applications. However, the wear behavior depends on the composition and microstructural design of the composite, which needs to be carefully studied and understood.

**Keywords:** metal–matrix composites; carbon nanotube composites; dual-matrix; powder processing; wear behavior



**Citation:** Abdeltawab, N.M.; Esawi, A.M.K.; Wifi, A. Investigation of the Wear Behavior of Dual-Matrix Aluminum–(Aluminum–Carbon Nanotube) Composites. *Metals* **2023**, *13*, 1167. <https://doi.org/10.3390/met13071167>

Academic Editors: Ludmil Drenchev and Mihail Kolev

Received: 30 May 2023

Revised: 14 June 2023

Accepted: 18 June 2023

Published: 23 June 2023



**Copyright:** © 2023 by the authors. Licensee MDPI, Basel, Switzerland. This article is an open access article distributed under the terms and conditions of the Creative Commons Attribution (CC BY) license (<https://creativecommons.org/licenses/by/4.0/>).

## 1. Introduction

Over the past two decades, aluminum–carbon nanotube (Al–CNT) composites have received the attention of many researchers due to their numerous promising applications [1,2]. Agglomeration of the CNTs has been highlighted as a key challenge that researchers have focused on. Mechanical milling combined with thermo–mechanical processing was found to lead to well-densified composites with favorable strength, hardness, and wear resistance properties [3–8]. Investigations of the tribological behavior of Al–CNT composites showed that adding CNTs to aluminum enhances the wear resistance of the matrix [9–20]. It has been proposed that the crushed CNTs on the worn surface form a carbon film that works as a solid lubricating film. The wear rate was found to be affected by the weight percent (wt.%) of CNTs as well as the friction conditions such as sliding speed and applied load. Wear rate investigations for Al–CNT composites showed that the wear rate decreased by

increasing both sliding speed and the wt.% of CNT and increased by increasing the applied load to a certain critical value, after which the relation was inverted [6,11,12]. Investigations by various researchers also reported enhanced hardness of Al–CNT composites. However, this increase in hardness was accompanied by a severe loss in ductility [11,13,14,21,22].

Dual-phase materials consisting of a soft and a hard phase have been used for years in wear applications due to their outstanding combination of desirable properties. One common example is the tungsten carbide–cobalt (WC–Co) composite. The hard WC phase provides excellent wear resistance, while the soft Co matrix provides toughness and reduced friction, making the composite ideal for use in wear applications such as cutting tools, milling inserts, and wear-resistant coatings. Dual-matrix composites are similar to dual-phase materials. Typically, the reinforcement phase is distributed throughout one matrix, then embedded in the other matrix. Such microstructural design has the advantage of combining enhanced strength, hardness, wear resistance, toughness, and ductility. Accordingly, dual-matrix composites have been increasingly investigated as potential materials for wear applications. Various reinforcements and volume fractions have been investigated. A major advantage is the ability to tailor the characteristics of both the matrix and the reinforced composites to achieve the desired performance [23–27]. A dual composite of WC–Co was developed by Fang et al. [28] by embedding fully dense, large WC–Co particles in a cobalt matrix. The new material was found to have higher fracture toughness at the same wear resistance compared to conventional WC–Co.

More recently, efforts to fabricate dual-matrix composites have continued to report enhanced properties. For example, significant enhancement in ductility and wear resistance was reported by Lakra et al. [29], who fabricated a dual-matrix composite consisting of Al–Al<sub>3</sub>Ti–Al<sub>2</sub>O<sub>3</sub> separated by ductile unmilled outer Al matrix. A study by Eltaher et al. [30] investigated the mechanical and wear resistance of dual-matrix Al–Mg/Al<sub>2</sub>O<sub>3</sub>. The Al<sub>2</sub>O<sub>3</sub> particles were first milled with Mg before mixing with Al, which ensured their uniform dispersion. The composite exhibited improved wear resistance and high hardness and compressive strength while maintaining a high ductility. Overall, these studies demonstrate the potential of dual-matrix materials for wear applications. However, further research is needed to optimize the fabrication and processing of dual-matrix materials and to investigate their performance in a range of wear applications.

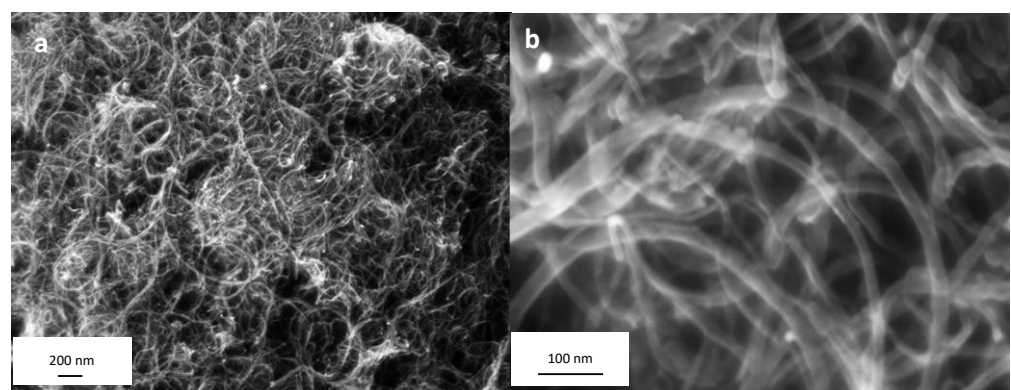
The investigation of Al–(Al–CNT) dual-matrix composites consisting of a primary matrix of soft aluminum in which milled hard particles of (Al–CNT) are dispersed was presented in previous work by Esawi and co-workers [31,32]. The Al–(Al–CNT) dual-matrix composites exhibited enhanced properties; however, the achieved enhancements depended on the mixing ratio between the reinforced particles and the soft Al matrix. For example, tensile test investigations showed that the highest tensile strength and elongation occur at a mixing ratio of 50%. Debonding between the hard reinforced phase and the soft Al limited further enhancements when using higher mixing ratios [32]. The wear and hardness properties of Al–(Al–CNT) dual-matrix composites were previously investigated by our research group for a composition of Al-5 wt.% CNT reinforced particles and 50% mixing ratio between reinforced particles to Al matrix equivalent to an overall CNT content of 2.5 wt.% [33]. The dual-matrix composites were compared with pure un-milled aluminum and single matrix Al-2.5 wt.% CNT. Results showed that the dual-matrix composites have better wear and hardness characteristics than pure un-milled aluminum but are lower than the single-matrix composite. It was proposed that the dual microstructure can be tailored by changing the mixing ratio of reinforced particles to aluminum matrix and wt.% CNT in the reinforced particles to obtain the optimized matrix composition at certain hardness and friction conditions for the required applications [33]. This motivates the present investigation.

In the present study, a more detailed investigation was carried out for hardness and wear rate using different compositions of Al–(Al–CNT) dual-matrix composites and various tribological conditions. A pin-on-disk test rig was used to investigate the wear rate against five control parameters: (1) wt.% CNT in the reinforced particles (C), (2) the mixing ratio

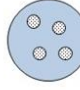
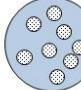
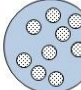
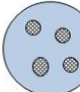
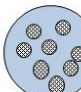
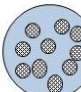
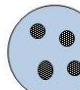
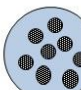
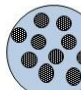
between the reinforced particles and the soft Al matrix (M), (3) sliding speed (S), (4) applied load (L), and (5) covered distance (D). To reveal the nonlinear effect of the parameters, each parameter was tested at three levels. A fractional statistical design based on the Taguchi approach was used to reduce the number of experiments [34,35]. Analysis of variance (ANOVA) was used to determine the significance of the control parameters and to derive mathematical regression models to model their effects on hardness and wear rate [36–40]. Response surface methodology (RSM) was used to represent the combined responses graphically. Scanning electron microscopy (SEM) was used to study the microstructure and to analyze the worn surfaces after the wear test in order to understand the wear mechanisms.

## 2. Materials and Methods

A Retsch® high energy planetary ball mill (PM400 MA-type) was used to produce 3, 4, and 5 wt.% Al–CNT composite powders. Gas-atomized ALPOCO® Al powder (purity > 99.7% and average particle size 75 µm) and Elicarb® MWCNTs (purity 70–90%, average diameter 10–12 nm, length tens of µm and density range 1.7–1.9 g/cm<sup>3</sup>, shown in Figure 1) were added in stainless steel milling jars of 250 mL volume, with 42 stainless steel milling balls of 10 mm diameter, and milled under Argon. Ball to powder ratio (BPR) of 5:1 and a milling speed of 400 rpm was used. The mixtures were milled for 1 h but interrupted every 10 min by a 20 min pause for cooling. High-purity ethyl alcohol supplied by SIGMA–ALDRICH® was used as a process control agent (PCA) with varying volumetric amounts relative to the CNT concentrations. For 3, 4, and 5 wt.% CNTs, the amount of ethyl alcohol used was 110, 70, and 50 µL, respectively. The milled Al–CNT powders were mixed with powders of unmilled pure Al using mechanical mixing in a Retsch® turbula mixer at a speed of 96 rpm for 30 min. Powders were prepared with mixing ratios of 25, 50, and 75% of reinforced particles to soft unreinforced Al. Figure 2 presents an illustration of the various dual-matrix microstructures prepared in the current study. The darker reinforced particles have higher CNT contents, and the larger number of particles in the microstructure represents higher mixing ratios. The mixed DM powders were subsequently compacted into 20 mm diameter compacts under a pressure of 350 MPa at room temperature for 1 h using a single-acting FOSTER® hydraulic press. The compacts were then sintered at a temperature of 500 °C for 1 h and extruded into 10 mm diameter rods. Finally, the die and the extrudate were covered by thermal insulation and left to cool slowly to room temperature.



**Figure 1.** (a) SEM image showing the morphology of the CNTs used in the current study. (b) Further magnification of the CNT sample shows CNTs with diameters ranging between 8 and 23 nm.

CNT% in reinforced particles	Mixing ratio		
	25%	50%	75%
3%	Overall CNT% 0.75 	Overall CNT% 1.5 	Overall CNT% 2.25 
	Overall CNT% 1 	Overall CNT% 2 	Overall CNT% 3 
	Overall CNT% 1.25 	Overall CNT% 2.5 	Overall CNT% 3.75 
4%			
5%			

**Figure 2.** Illustration of the dual-matrix microstructures investigated in the current study.

Hardness was evaluated for nine compositions according to Taguchi L<sub>9</sub> orthogonal array using Vickers hardness tester HV-50A (Vickers, London, UK) under an applied load of 10 N and dwell time of 10 s. Five readings were taken for each sample, and three samples were investigated for each composition. Wear rate investigations were carried out according to ASTM G99-95 Standard Test Method for wear [41]. The apparatus used was Plint TE/P indexing Pin-on-Disk with a steel disk (EN31 high chrome tool steel) of hardness 25 HRC. The wear specimen (pin) of 8 mm diameter and 20 mm height was cut from the extruded rods, machined, and polished metallographically to ensure surface roughness is below 0.8  $\mu\text{m}$ . The mass of the pin was recorded before and after the test, and the wear rate was calculated as mass loss per second ( $\mu\text{g/s}$ ). The tangential force due to friction was recorded using a load cell attached to the arm that carries the pin, where the coefficient of friction (COF) was calculated as the ratio between the normal load acting on the pin to the tangential force. LEO SUPRA 55-Field Emission Scanning Electron Microscope (SEM, Zeiss, Selangor, Malaysia) was used to investigate the sample's microstructure and worn surfaces after the wear test.

Wear investigation was conducted for five control parameters, with each having three level values (Table 1) according to Taguchi L<sub>27</sub> orthogonal array ( $3^{13}$ ) (Table 2) [40]. The wear rate was recorded for three replicates at each sample condition. To study the effect of the control parameters in maximizing or minimizing the response, the signal-to-noise ratio (S/N) was calculated. ANOVA analysis was used to determine the significance of each control parameter [42–45]. A mathematical regression model was built to capture the effects of the control parameters on the response [34]. The model was used to plot response surfaces that represent the combined effects of the control parameters on the wear rate [42,46,47].

**Table 1.** Levels of control parameters for wear rate investigation.

Control Variables	Symbol	Level 1	Level 2	Level 3
wt.% CNT in reinforced matrix	C	3	4	5
Linear speed of pin on disk (m/s)	S	0.5	1	1.5
Load applied on pin (N)	L	8	14	20
Distance covered by pin against disk (Km)	D	0.6	1	1.4
Mixing ratio of reinforced to unreinforced particles	M	25	50	75



**Table 2.** Layout of the  $L_{27}$  orthogonal array.

Sample No.	CNT (%)	Speed (m/s)	Load (N)	Distance (Km)	Mixing Ratio (%)
1	3	0.5	8	0.6	25
2	3	0.5	14	1	50
3	3	0.5	20	1.4	75
4	3	1	8	1	75
5	3	1	14	1.4	25
6	3	1	20	0.6	50
7	3	1.5	8	1.4	50
8	3	1.5	14	0.6	75
9	3	1.5	20	1	25
10	4	0.5	8	0.6	25
11	4	0.5	14	1	50
12	4	0.5	20	1.4	75
13	4	1	8	1	75
14	4	1	14	1.4	25
15	4	1	20	0.6	50
16	4	1.5	8	1.4	50
17	4	1.5	14	0.6	75
18	4	1.5	20	1	25
19	5	0.5	8	0.6	25
20	5	0.5	14	1.4	50
21	5	0.5	20	1.4	75
22	5	1	8	1	75
23	5	1	14	1.4	25
24	5	1	20	0.6	50
25	5	1.5	8	1.4	50
26	5	1.5	14	0.6	75
27	5	1.5	20	1	25

### 3. Results and Discussion

Figure 3a presents the typical microstructure of Al–(Al–CNT) dual-matrix composites showing both the unreinforced Al (dark phase) and the reinforced Al–CNT (light phase). Upon further magnification, as in Figure 3b, the Al grains are seen to have large uniform sizes, whereas the milled reinforced phase is composed of small scattered particles. It is also apparent that the sintering temperature was sufficient for consolidating the aluminum while preserving the small grain sizes of the milled particles.

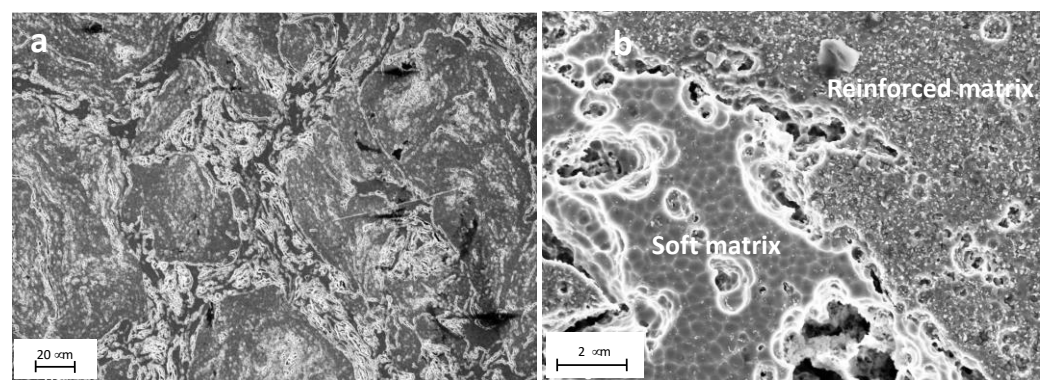


**Figure 3.** (a) Typical microstructure of Al–(Al–CNT) dual-matrix composites of Al-4 wt.% CNT and 75% mixing ratio. (b) Further magnification.

#### 3.1. Hardness Investigation

As presented in Figure 4, hardness increases with the increase of mixing ratio and wt.% CNT in the reinforced particles (and, accordingly, the overall wt.% CNT in the composite).

The maximum hardness (66.55 HV) occurred at the composition of Al-5 wt.% CNT in reinforced particles and a mixing ratio of 75%, whereas minimum hardness (25.56 HV) occurred for the composition of Al-3 wt.% CNT in reinforced particles and mixing ratio of 25%. ANOVA analysis of the S/N ratio was conducted to determine the significance of each parameter in maximizing hardness. The results showed that the mixing ratio (M) is the most significant parameter that increases hardness. This was followed by the wt.% CNT in the reinforced particles (C). Using regression analysis, Equation (1) was obtained to express the relation between Vickers hardness (HV) and the significant control variables: mixing ratio (M) and wt.% CNT in reinforced particles (C). With regards to the microhardness of the various regions in the samples, the current authors presented in an earlier publication [33] that the average micro-hardness of the pure Al unmilled zone was 57.5 HV, whereas that of the Al-5 wt.% CNT zone was 65.6 HV and have noted that both values are lower than those for samples made entirely of either pure unmilled Al or single matrix samples with 5 wt.% CNT. The lower hardness of the different regions in the dual-matrix material is attributed to the effect of the interaction with the neighboring hard/soft phase as well as the strength of the interface between them.

$$HV = 42.23 - 12.303C - 0.227M + 1.494C^2 + 0.0002M^2 + 0.187M * C \quad (1)$$

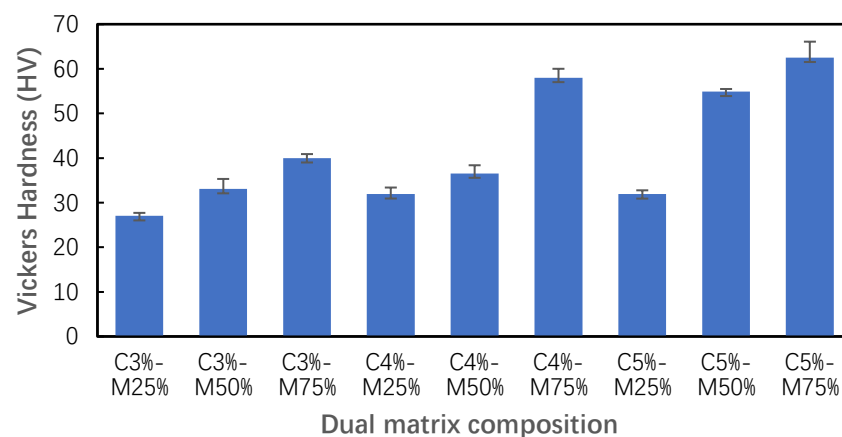


**Figure 4.** Hardness results of Al–(Al–CNT) dual-matrix composites.

### 3.2. Wear Investigation

Wear rates and COF of the Al–(Al–CNT) dual-matrix composites are presented in Figures 5 and 6, respectively. The lowest wear rate ( $WR = 12.6 \mu\text{g/s}$ ) and coefficient of friction ( $\text{COF} = 0.384$ ) were observed for sample no.7 ( $C = 3\%$ ,  $M = 50\%$ ,  $S = 1.5 \text{ m/s}$ ,  $L = 8 \text{ N}$ , and  $D = 1.4 \text{ Km}$ ). It is worth noting that, according to the hardness investigation, this sample has an average hardness of 33 HV, which is about half of the hardness of some of the other tested samples. Accordingly, the sample has the advantage of combining high wear resistance with good formability, which is typically difficult to achieve. The worn surface of the sample is presented in Figure 7a and shows a smooth surface with shallow grooves. No debris was observed. The governing wear mechanism appears to be adhesive wear with smeared layers that indicate the presence of plastic deformation. Further magnification in Figure 7b shows that the reinforced matrix has a flat surface where CNT is believed to have worked effectively as a lubricant. The COF time plot presented in Figure 8 shows low variation in COF values reflecting smooth sliding. This is believed to be due to the lubricating effect of the CNTs in the reinforced particles.

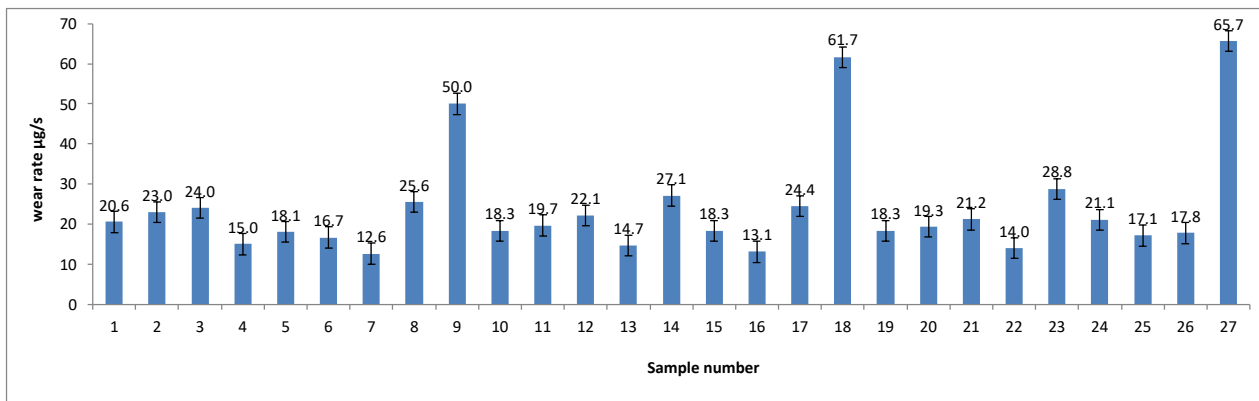


**Figure 5.** Wear rate results of dual-matrix Al-(Al-CNT) composites.

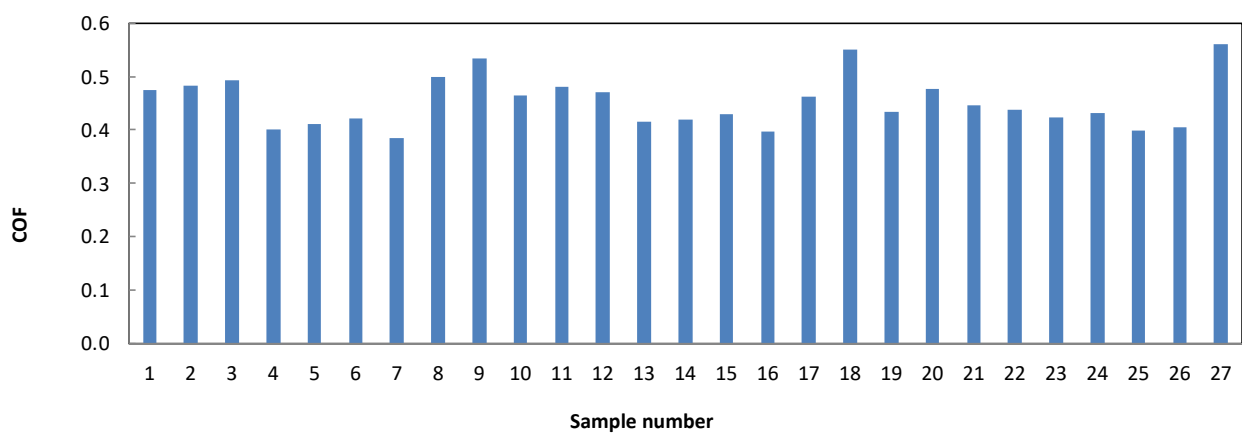


**Figure 6.** Average COF results of dual-matrix Al-(Al-CNT) composites.

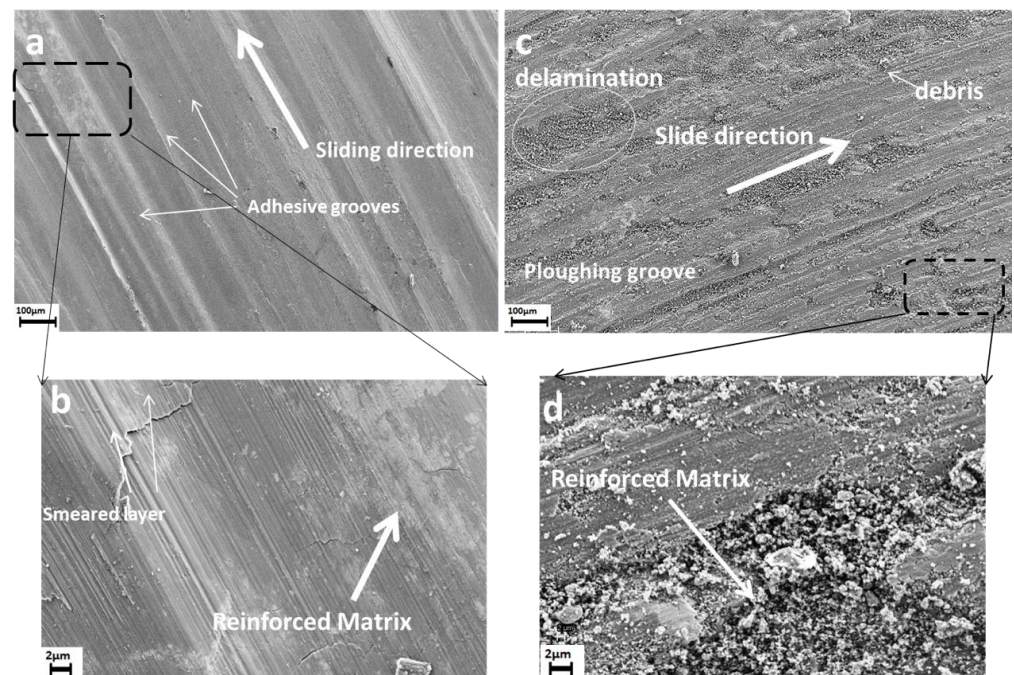


**Figure 7.** SEM worn surfaces for samples with (a) the lowest wear rate (sample 7: C3%, M50%, D1.4 Km, L8 N, S1.5 m/s), (c) the highest wear rate (sample 27: C5%, M25%, D1 Km, L20 N, S1.5 m/s), (b,d) are magnified images of (a,c).



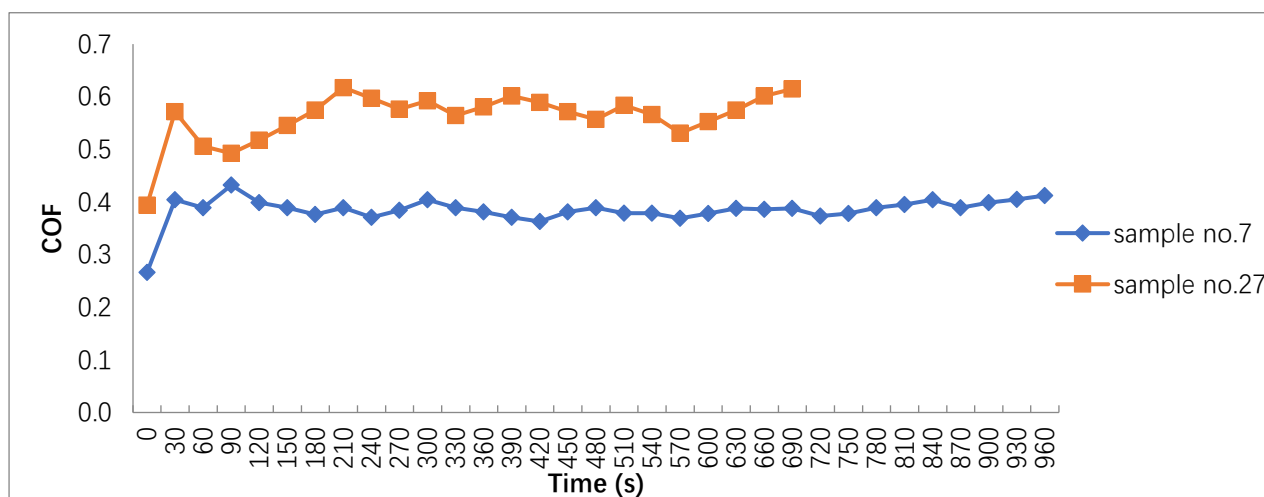


**Figure 8.** COF time plot of sample no.7 (lowest wear rate sample: C3%, M50%, D1.4 Km, L8 N, S1.5 m/s) and COF time plot of sample no.27 (highest wear rate sample: C5%, M25%, D1 Km, L20 N, S1.5 m/s).

On the other hand, the highest wear rate ( $WR = 65.7 \mu\text{g/s}$ ) and COF (0.561) occurred for sample no.27 ( $C = 5\%$ ,  $M = 25\%$ ,  $S = 1.5 \text{ m/s}$ ,  $L = 20 \text{ N}$ , and  $D = 1 \text{ Km}$ ). The worn surface of the sample presented in Figure 7c shows deep grooves, and the dominant wear mechanism appears to be abrasive with the presence of delamination and cracks on the surface. Further magnification in Figure 7d shows that fragmentation occurred in the reinforced matrix, with the resulting hard debris causing abrasive wear. The COF time plot of sample no.27 presented in Figure 8 shows intensive fluctuation reflecting the severe fragmentation of the reinforced particles. It is worth noting that samples no.9 and 18 also demonstrate higher wear rates than all other tested samples, as can be clearly noticed from Figure 5. Both samples have 25% mixing ratio which is similar to sample no.27 and were tested under similar conditions to sample no.27 ( $S = 1.5 \text{ m/s}$ ,  $L = 20 \text{ N}$ , and  $D = 1 \text{ Km}$ ). The only difference is the lower composition of the CNT in the reinforced particles, which is 3% and 4% in samples no.9 and 18, respectively, compared to 5% in sample no.27.

ANOVA analysis revealed that the applied load ( $L$ ) is the most effective parameter in increasing the wear rate. Figure 9 presents further analysis of the effect of load on the interface between the Al-CNT reinforced matrix and the Al matrix. At the highest load of 20 N in Figure 9a, the reinforced matrix is exposed to high fragmentation that appears to reduce its lubricating effect. In addition, the wear mechanism turns abrasive. At the applied load of 14 N in Figure 9b, the reinforced matrix has surface cracks. On the other hand, at an applied load of 8 N in Figure 9c, the reinforced matrix is completely flat, and the CNT works as a lubricant. The mixing ratio ( $M$ ) is found to be the next effective parameter. It was found that the wear rate decreases at ( $M$ ) from 25% to 50%, but then it increases at ( $M$ ) from 50% to 75%. Local plowing resulting in pulled-out areas on the surface at a 75% mixing ratio was observed. Typically worn surfaces showing pulled areas are presented in Figure 10a,b for sample no.4 and sample no.17, respectively. It is believed that the high difference in hardness between the reinforced matrix and the Al matrix caused the interface between them to be weak, that in turn facilitated the pull-out of the reinforced matrix even at low loads. Tensile strength investigations of dual-matrix Al-(Al-CNT) composites were conducted in another study by our research group and showed that composites with a mixing ratio of 75% have lower strength than dual-matrix composites with a 50% mixing ratio. This was attributed to the weaker interface associated with the larger overall interfacial area as the number of reinforced particles in the matrix increases [32].

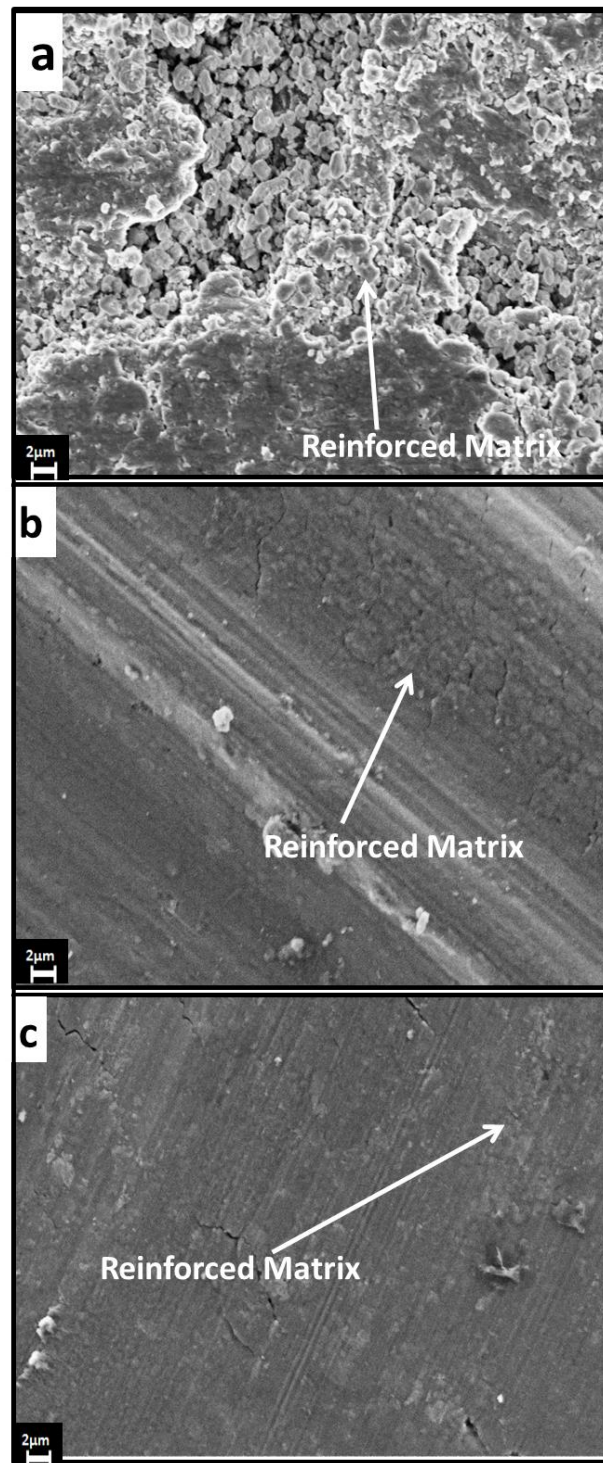


**Figure 9.** Typical micrograph of the worn surfaces at the interface between the Al and reinforced matrix under different loads: (a) sample no.3 (C3%, M75%, D1.4 Km, L20 N, S0.5 m/s), (b) sample no.2 (C3%, M50%, D1 Km, L14 N, S0.5 m/s, and (c) sample no.1 (C3%, M25%, D1.4 Km, L8 N, S0.5 m/s).

The linear speed (S) comes next in significance. The wear rate was found to decrease at (S) from 0.5 m/s to 1 m/s, but then it increased from 1 m/s to 1.5 m/s. While the wear rate of Al-CNT single matrix composites was reported to decrease as linear speed increases [11], in the present study, the behavior of the dual-matrix composites was found to be different. The distance covered (D) was also observed to influence the wear rate, which was found to

increase from 0.6 Km to 1 Km and then decrease from 1 Km to 1.4 Km. This could be due to the strain-hardening of the worn surfaces as the distance covered increases which are believed to reduce the wear rate. Lastly, it was found that the CNT wt.% (C) has minimal effect in the case of the dual-matrix composites studied, which is distinctively different from Al–CNT single matrix composites. This is assumed to be due to the more dominating effect of the mixing ratio. It is believed that the hard reinforced particles form islands of high wear resistance within the soft Al matrix, as we reported in an earlier study [33], with the overall wear resistance being influenced by the number of such particles.

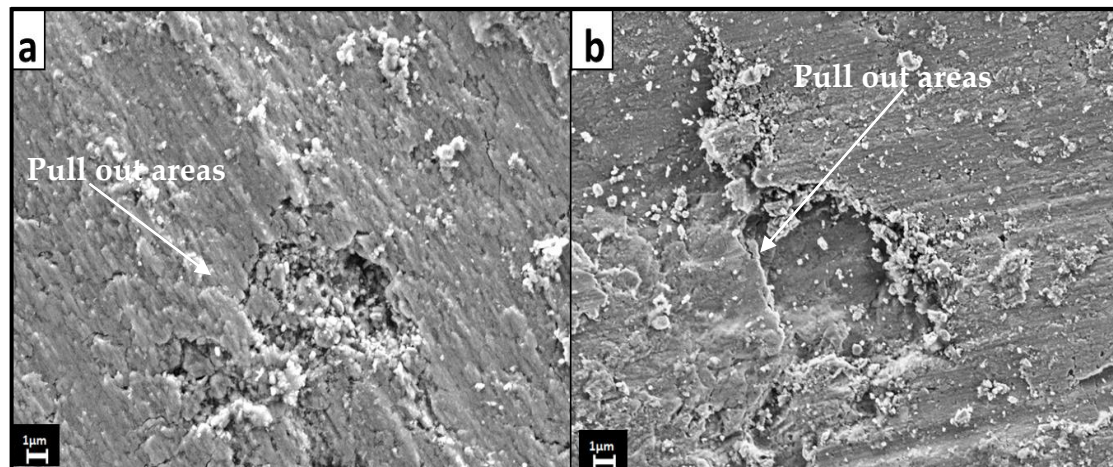


**Figure 10.** Pull-out areas in a reinforced matrix at a mixing ratio of 75% (a) sample no.4 (C3%, M75%, D1 Km, L8 N, S1 m/s) and (b) sample no.17 (C4%, M75%, D0.6 Km, L8 N, S1.5 m/s).

A mathematical regression model expressing the relation between the wear rate and the significant parameters is presented in Equation (2). A three-dimensional response surface graph is plotted in Figure 11a to represent the relation between wear rate and load- speed. It shows that the relation is proportional (as speed and load increase, the wear rate increases). The lowest wear rate occurs at levels of about 8 N and 0.8 m/s for load and speed, respectively. The relation between the wear rate and the speed-mixing ratio is presented in Figure 11b, where it is shown that the lowest wear rate occurs at levels of about 0.8 m/s and 57% for speed and mixing ratio, respectively. The relation between wear rate and speed-distance is presented in Figure 11c, where the lowest wear rate occurs at about 0.8 m/s and 0.6 Km, respectively. It can be observed that the minimum wear rate takes place at 0.6 Km and that the surface concaved up at a covered distance of 1 KM, then it inverted down again. This can be attributed to strain-hardening of the worn surfaces. Finally, the relation between wear rate and the load-mixing ratio is shown in Figure 11d, where the lowest wear rate occurs at levels 8 N and 57% for load and mixing ratio, respectively.

$$WR = 8.095 - 45.146 S - 0.14 L + 139.794 D - 1.7 M + 28.205 S^2 + 0.057 L^2 - 69.6 D^2 + 0.015 M^2 \quad (2)$$

Response surfaces graphs show that increasing speed over 1 m/s increases the wear rate; where it was observed during wear investigations that increasing the speed causes noise and vibrations in the system leading to high variations in the COF time plot. Figure 12 shows the COF time plot of a sample exposed to a higher speed. It is clear that the response is rougher than an equivalent sample exposed to a lower speed. Analysis of the worn surfaces of the two samples in Figure 13 shows that the crushed reinforced area is bigger at higher speeds and that the crushed particles changed to debris, which increased the severity of the abrasion wear.

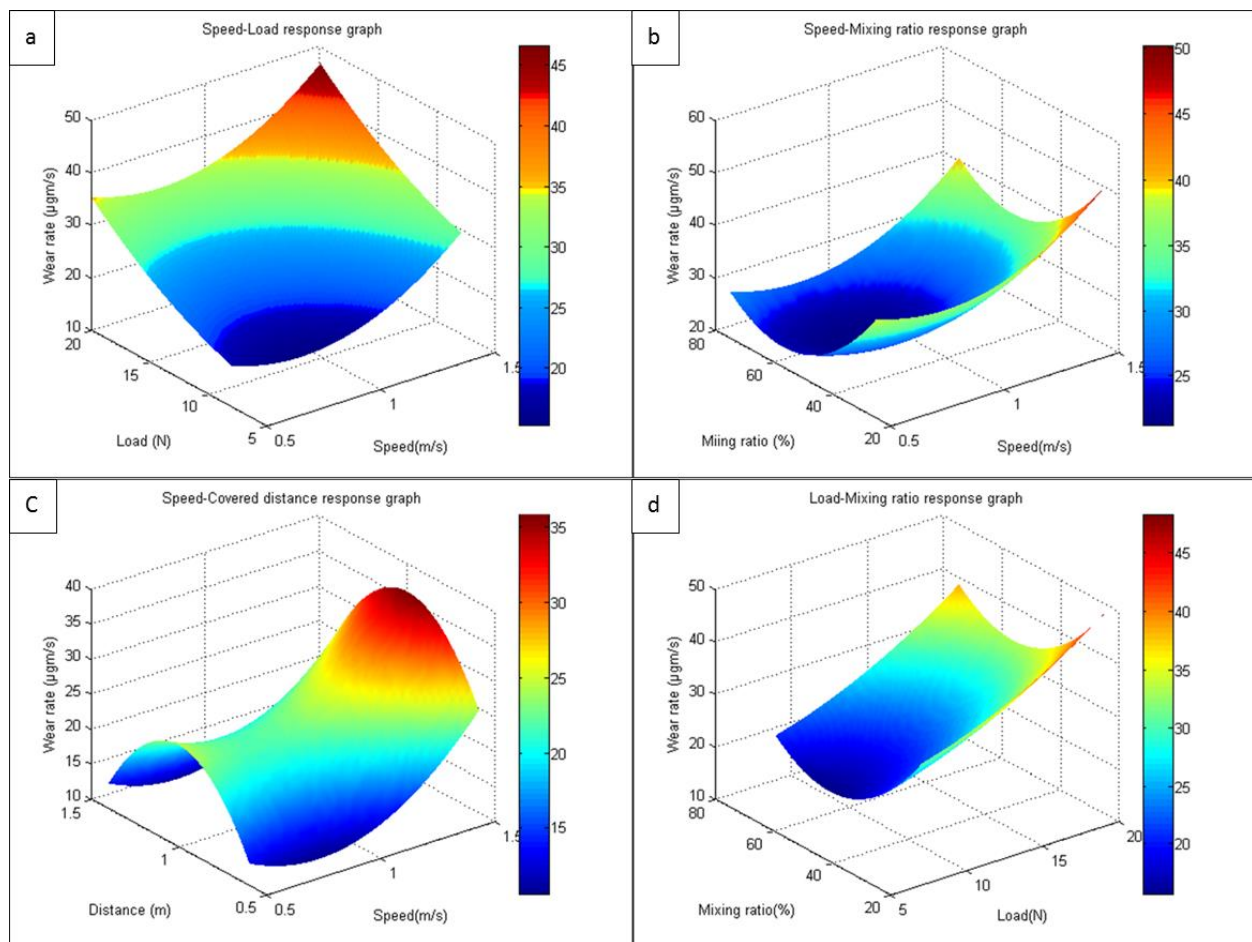


**Figure 11.** (a–d) Response surface graphs of the combined effects of the control parameters on the wear rate.

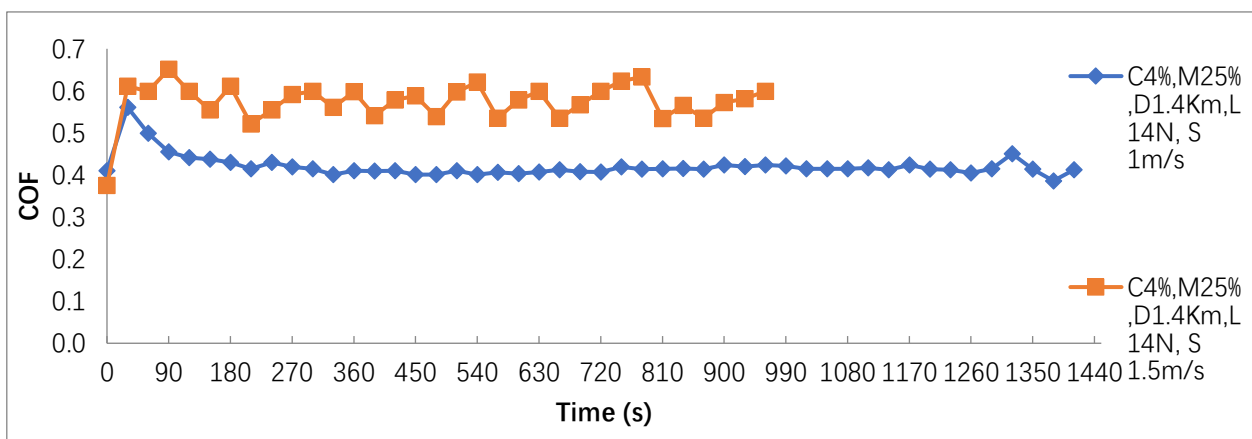


**Figure 12.** Effect of speed on COF time plot of sample (C4%, M25%, D1.4 Km, L14 N).



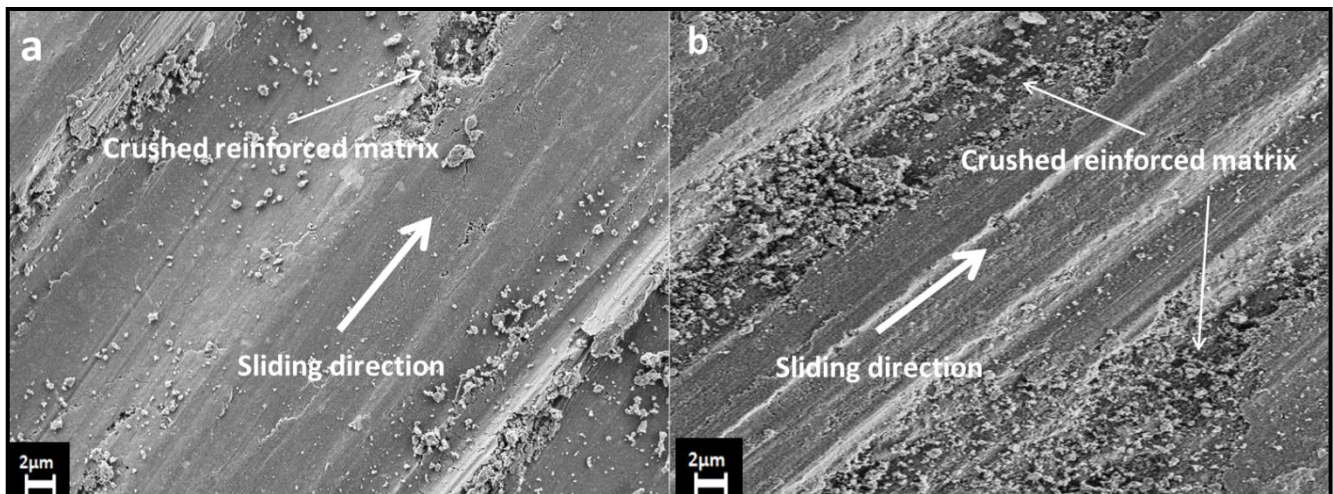


**Figure 13.** Effect of speed on worn surfaces of (a) sample (C4%, M25%, D1.4 Km, L14 N, 1 m/s) and (b) sample (C4%, M25%, D1.4 Km, L14 N, 1.5 m/s).

#### 4. Conclusions

The current study investigated the effect of several factors, namely, wt.% CNT, mixing ratio, sliding speed, applied load, and covered distance on hardness and wear rate of Al–(Al–CNT) dual-matrix composites. It was found that the mixing ratio is significant in impacting the wear behavior of DM Al–(Al–CNT) composites. A mixing ratio of 50% and a CNT content of 3 wt.% at the lowest applied load were found to give the lowest wear rate and coefficient of friction, according to our experiments. A significant reduction in wear rate of up to 80.8% was achieved under such conditions. This was attributed to the novel dual-matrix design in which the harder, more wear-resistant reinforced phase formed islands within the softer phase and have accordingly strongly influenced the overall wear behavior of the composite. In addition to the tested conditions, our model predicted that decreasing the mixing ratio below a critical value of 57% would increase the wear rate.

The multifactorial experimental study, which combined the effects of parameters related to the composite itself (wt.% CNT and mixing ratio between the reinforcement particles and the Al matrix), as well as parameters related to the wear process (sliding speed, applied load, and distance), showed that the dual-matrix microstructural design is very promising for wear applications provided that the reinforced matrix is kept consolidated and not fragmented under the applied friction condition. As conditions become more severe, fragmentation in the reinforced matrix occurs at the interface between it and the soft matrix and progresses to severe plowing of the reinforced area, especially at high mixing ratios. Both adhesive and abrasive wear mechanisms were observed depending on the material composition and the test conditions. However, because of the hard reinforcement phase and the fragmentation which occurred, abrasive wear appeared to be more dominant. In addition to understanding the complex wear mechanisms, true COF dependence on the hardness difference between the friction pairs, which has recently been reported to have a major influence on the tribological behavior of AA7075–TiB<sub>2</sub> nanocomposites, can further enhance the understanding of the performance of dual-matrix composites in various wear applications [48].

Overall, the wear resistance of Al–(Al–CNT) dual-matrix composites can be further improved through the optimization of the matrix and reinforcement phase, control of the distribution and size of the reinforcement phase, strengthening the interface between the Al matrix and the Al–CNT composite, and optimization of the processing parameters during the composite fabrication in order to reach a balance between strength and ductility in the reinforced particles while still ensuring uniform dispersion of the CNTs.



**Author Contributions:** Conceptualization, A.M.K.E. and A.W.; methodology, A.M.K.E. and A.W.; literature search, N.M.A.; validation, N.M.A.; investigation, N.M.A.; data collection, N.M.A.; data analysis, N.M.A., A.M.K.E. and A.W.; data interpretation, N.M.A., A.M.K.E. and A.W.; writing—original draft preparation, N.M.A.; writing—review and editing, A.M.K.E. and A.W.; supervision, A.M.K.E. and A.W. All authors have read and agreed to the published version of the manuscript.

**Funding:** This research received no external funding.

**Institutional Review Board Statement:** Not applicable.

**Informed Consent Statement:** Not applicable.

**Acknowledgments:** A.M.K. Esawi wishes to acknowledge the financial support by the American University in Cairo (AUC), Egypt. Special thanks to Emy, Noura and Jameela E. for continuous support.

**Conflicts of Interest:** The authors declare no conflict of interest.

## References

1. Nieto, A.; Agarwal, A.; Lahiri, D.; Bisht, A.; Bakshi, S.R. *Carbon Nanotubes: Reinforced Metal Matrix Composites*; CRC Press: Boca Raton, FL, USA, 2021.
2. Yue, Y.; Zhou, L.; Li, M.; Xu, F.; Cai, X. Research Progress on Microstructure Design of CNTs Reinforced Al Matrix Composites. *Integr. Ferroelectr.* **2023**, *234*, 22–32. [\[CrossRef\]](#)
3. Esawi, A.; Morsi, K. Dispersion of carbon nanotubes (CNTs) in aluminum powder. *Compos. Part A Appl. Sci. Manuf.* **2007**, *38*, 646–650. [\[CrossRef\]](#)
4. Raviathul Basariya, M.; Srivastava, V.C.; Mukhopadhyay, N.K. Microstructural characteristics and mechanical properties of carbon nanotube reinforced aluminum alloy composites produced by ball milling. *Mater. Des.* **2014**, *64*, 542–549. [\[CrossRef\]](#)
5. Hao, X.-N.; Zhang, H.-P.; Zheng, R.-X.; Zhang, Y.-T.; Ameyama, K.; Ma, C.-L. Effect of mechanical alloying time and rotation speed on evolution of CNTs/Al-2024 composite powders. *Trans. Nonferrous Met. Soc. China* **2014**, *24*, 2380–2386. [\[CrossRef\]](#)
6. Omid, M.; Khodabandeh, A.; Nategh, S.; Khakbiz, M. Microstructural and tribological properties of nanostructured Al6061-CNT produced by mechanical milling and extrusion. *Adv. Powder Technol.* **2018**, *29*, 543–554. [\[CrossRef\]](#)
7. George, R.; Kashyap, K.T.; Rahul, R.; Yamdagni, S. Strengthening in carbon nanotube/aluminium (CNT/Al) composites. *Scr. Mater.* **2005**, *53*, 1159–1163. [\[CrossRef\]](#)
8. Jafari, M.; Abbasi, M.H.; Enayati, M.H.; Karimzadeh, F. Mechanical properties of nanostructured Al2024–MWCNT composite prepared by optimized mechanical milling and hot pressing methods. *Adv. Powder Technol.* **2012**, *23*, 205–210. [\[CrossRef\]](#)
9. Pérez-Bustamante, R.; Bueno-Escobedo, J.L.; Jiménez-Lobato, J.; Estrada-Guel, I.; Miki-Yoshida, M.; Licea-Jiménez, L.; Martínez-Sánchez, R. Wear behavior in Al2024–CNTs composites synthesized by mechanical alloying. *Wear* **2012**, *292–293*, 169–175. [\[CrossRef\]](#)
10. Al-Qutub, A.M.; Khalil, A.; Saheb, N.; Hakeem, A.S. Wear and friction behavior of Al6061 alloy reinforced with carbon nanotubes. *Wear* **2013**, *297*, 752–761. [\[CrossRef\]](#)
11. Bastwros, M.M.H.; Esawi, A.M.K.; Wifi, A. Friction and wear behavior of Al–CNT composites. *Wear* **2013**, *307*, 164–173. [\[CrossRef\]](#)
12. Abdullahi, U.; Maleque, M.A.; Nirmal, U. Wear Mechanisms Map of CNT–Al Nano-composite. *Procedia Eng.* **2013**, *68*, 736–742. [\[CrossRef\]](#)
13. Piasecki, A.; Paczos, P.; Tuliński, M.; Kotkowiak, M.; Popławski, M.; Jakubowicz, M.; Wieczorowski, M. Microstructure, mechanical properties and tribological behavior of Cu-nano TiO<sub>2</sub>-MWCNTs composite sintered materials. *Wear* **2023**, *522*, 204834. [\[CrossRef\]](#)
14. Aydin, F. The investigation of the effect of particle size on wear performance of AA7075/Al<sub>2</sub>O<sub>3</sub> composites using statistical analysis and different machine learning methods. *Adv. Powder Technol.* **2021**, *32*, 445–463. [\[CrossRef\]](#)
15. Abbasipour, B.; Niroumand, B.; Vaghefi, S.M.M.; Abedi, M. Tribological behavior of A356–CNT nanocomposites fabricated by various casting techniques. *Trans. Nonferrous Met. Soc. China* **2019**, *29*, 1993–2004. [\[CrossRef\]](#)
16. Manjunath Naik, H.R.; Manjunath, L.H.; Malik, V.; Manjunath Patel, G.C.; MeSaxena, K.K.; Lakshmikanthan, A. Effect of microstructure, mechanical and wear on Al-CNTs/graphene hybrid MMC'S. *Adv. Mater. Process. Technol.* **2022**, *8* (Suppl. S2), 366–379.
17. Srinivas, V.; Jayaraj, A.; Venkataramana, V.S.N.; Avinash, T.; Dhanyakanth, P. Effect of ultrasonic stir casting technique on mechanical and tribological properties of aluminium–multi-walled carbon nanotube nanocomposites. *J. Bio-Tribo-Corros.* **2020**, *6*, 3. [\[CrossRef\]](#)
18. Sahoo, B.; Narsimhachary, D.; Paul, J. Surface mechanical and self-lubricating properties of MWCNT impregnated aluminium surfaces. *Surf. Eng.* **2019**, *35*, 970–981. [\[CrossRef\]](#)
19. Kumar, L.; Alam, S.N.; Sahoo, S.K. Influence of nanostructured Al on the mechanical properties and sliding wear behavior of Al-MWCNT composites. *Mater. Sci. Eng. B* **2021**, *269*, 115162. [\[CrossRef\]](#)
20. Kumar, R.; Bhowmick, H.; Gupta, D.; Bansal, S. Development and characterization of multiwalled carbon nanotube-reinforced microwave sintered hybrid aluminum metal matrix composites: An experimental investigation on mechanical and tribological performances. *Proc. Inst. Mech. Eng. Part L J. Mater. Des. Appl.* **2021**, *23*, 2310–2323. [\[CrossRef\]](#)

21. Bradbury, C.R.; Gomon, J.-K.; Kollo, L.; Kwon, H.; Leparoux, M. Hardness of Multi Wall Carbon Nanotubes reinforced aluminium matrix composites. *J. Alloy. Compd.* **2014**, *585*, 362–367. [\[CrossRef\]](#)
22. Morsi, K.; Esawi, A.M.K.; Lanka, S.; Sayed, A.; Taher, M. Spark plasma extrusion (SPE) of ball-milled aluminum and carbon nanotube reinforced aluminum composite powders. *Compos. Part A Appl. Sci. Manuf.* **2010**, *41*, 322–326. [\[CrossRef\]](#)
23. Runkle, J.C. Method for Making Tool Steel with High Thermal Fatigue Resistance. U.S. Patent 5,290,507, 1 March 1994.
24. Odeshi, A.G.; Mucha, H.; Wielage, B. Manufacture and characterisation of a low cost carbon fibre reinforced C/SiC dual matrix composite. *Carbon* **2006**, *44*, 1994–2001. [\[CrossRef\]](#)
25. Morsi, K.; Patel, V.V.; Naraghi, S.; Garay, J.E. Processing of titanium–titanium boride dual matrix composites. *J. Mater. Process. Technol.* **2008**, *196*, 236–242. [\[CrossRef\]](#)
26. Deng, X.; Patterson, B.; Chawla, K.; Koopman, M.; Mackin, C.; Fang, Z.; Lockwood, G.; Griffo, A. Microstructure/hardness relationship in a dual composite. *J. Mater. Sci. Lett.* **2002**, *21*, 707–709. [\[CrossRef\]](#)
27. Patel, V.V.; El-Desouky, A.; Garay, J.E.; Morsi, K. Pressure-less and current-activated pressure-assisted sintering of titanium dual matrix composites: Effect of reinforcement particle size. *Mater. Sci. Eng. A* **2009**, *507*, 161–166. [\[CrossRef\]](#)
28. Fang, Z.; Lockwood, G.; Griffo, A. A Dual composite of WC-Co. *Metall. Mater. Trans. A* **1999**, *30*, 3231–3238. [\[CrossRef\]](#)
29. Lakra, S.; Bandyopadhyay, T.K.; Das, S.; Das, K. Synthesis and characterization of in-situ (Al<sub>3</sub>Al<sub>2</sub>O<sub>3</sub>)/Al dual matrix composite. *J. Alloy. Compd.* **2020**, *842*, 155745. [\[CrossRef\]](#)
30. Eltaher, M.A.; Wagih, A.; Melaibari, A.; Fathy, A.; Lubineau, G. Effect of Al<sub>2</sub>O<sub>3</sub> particles on mechanical and tribological properties of Al–Mg dual-matrix nanocomposites. *Ceram. Int.* **2020**, *46*, 5779–5787. [\[CrossRef\]](#)
31. Esawi, A.; Morsi, K.; Salama, I.; Saleeb, H. Processing Challenges of Dual-Matrix Carbon Nanotube Aluminum Composites. In Proceedings of the "Randall M. German Honorary Symposium on Sintering and Powder-Based Materials", TMS Spring Conference, Orlando, FL, USA, 11–15 March 2012; Volume 1, pp. 545–552.
32. Salama, E.I.; Abbas, A.; Esawi, A.M.K. Preparation and properties of dual-matrix carbon nanotube-reinforced aluminum composites. *Compos. Part A Appl. Sci. Manuf.* **2017**, *99*, 84–93. [\[CrossRef\]](#)
33. Bastwros, M.M.H.; Esawi, A.M.K.; Wifi, A. Tribological behavior of dual matrix Al-CNT Composites, In Proceedings of the JSME/ASME 2014 International Conference on Materials and Processing (ICMP2014), Detroit, Michigan, USA, 9–13 June 2014.
34. Montgomery, D.C. *Design and Analysis of Experiments*; John Wiley & Sons: Hoboken, NJ, USA, 2008.
35. Maghsoodloo, S.; Ozdemir, G.; Jordan, V.; Huang, C.-H. Strengths and limitations of taguchi's contributions to quality, manufacturing, and process engineering. *J. Manuf. Syst.* **2004**, *23*, 73–126. [\[CrossRef\]](#)
36. Kumar, R.; Dhiman, S. A study of sliding wear behaviors of Al-7075 alloy and Al-7075 hybrid composite by response surface methodology analysis. *Mater. Des.* **2013**, *50*, 351–359. [\[CrossRef\]](#)
37. El-Tayeb, N.; Yap, T.; Brevern, P. Wear characteristics of titanium alloy Ti54 for cryogenic sliding applications. *Tribol. Int.* **2010**, *43*, 2345–2354. [\[CrossRef\]](#)
38. Gajjal, S.Y.; Unkule, A.J.; Gajjal, P.S. Taguchi Technique for Dry Sliding Wear Behavior of PEEK Composite Materials. *Mater. Today Proc.* **2018**, *5*, 950–957. [\[CrossRef\]](#)
39. Ghalme, S.; Mankar, A.; Bhalerao, Y. Integrated Taguchi-simulated annealing (SA) approach for analyzing wear behaviour of silicon nitride. *J. Appl. Res. Technol.* **2017**, *15*, 624–632. [\[CrossRef\]](#)
40. Taguchi, G.; Konishi, S. *Orthogonal Arrays and Linear Graphs: Tools for Quality Engineering*; American Supplier Institute: Cairo, Egypt, 1987.
41. Standard, A. G99, *Standard Test Method for Wear Testing with a Pin-on-Disk Apparatus*; ASTM International: West Conshohocken, PA, USA, 2006.
42. Baskaran, S.; Anandakrishnan, V.; Duraiselvam, M. Investigations on dry sliding wear behavior of in situ casted AA7075–TiC metal matrix composites by using Taguchi technique. *Mater. Des.* **2014**, *60*, 184–192. [\[CrossRef\]](#)
43. Singh, S.K.; Sudeepan, J.; Kumar, K.; Barman, T.K.; Sahoo, P. Study of Friction and Wear of ABS/ZnO Polymer Composite Using Taguchi Technique. *Procedia Mater. Sci.* **2014**, *6*, 391–400.
44. Joshi, A.Y.; Patel, V.N.; Banker, V.J.; Mistry, J.M.; Thakor, M.R.; Upadhyay, B.H. Wear Behavior in Dry Sliding of Inconel 600 Alloy Using Taguchi Method and Regression Analysis. *Procedia Technol.* **2016**, *23*, 383–390.
45. Singh, S.K.; Zakaulla, M.; Khan, A.R.A.; Mukunda, P.G. Evaluation of the Taguchi Method for Wear Behavior of Al6061/Cu–SiC/Cu–Gr Hybrid Composite. *Mater. Today Proc.* **2015**, *2*, 2951–2958.
46. Murugan, K.; Ragupathy, A.; Balasubramanian, V.; Sridhar, K. Optimizing HVOF spray process parameters to attain minimum porosity and maximum hardness in WC–10Co–4Cr coatings. *Surf. Coat. Technol.* **2014**, *247*, 90–102. [\[CrossRef\]](#)
47. Kiran, T.S.; Kumar, M.P.; Basavarajappa, S.; Viswanatha, B.M. Dry sliding wear behavior of heat treated hybrid metal matrix composite using Taguchi techniques. *Mater. Des.* **2014**, *63*, 294–304. [\[CrossRef\]](#)
48. Pan, S.; Saso, T.; Yu, N.; Sokoluk, M.; Yao, G.; Umehara, N.; Li, X. New study on tribological performance of AA7075–TiB<sub>2</sub> nanocomposites. *Tribol. Int.* **2020**, *152*, 106565. [\[CrossRef\]](#)

**Disclaimer/Publisher's Note:** The statements, opinions and data contained in all publications are solely those of the individual author(s) and contributor(s) and not of MDPI and/or the editor(s). MDPI and/or the editor(s) disclaim responsibility for any injury to people or property resulting from any ideas, methods, instructions or products referred to in the content.